Molecular Characterization of NikD, a New Flavoenzyme Important in the Biosynthesis of Nikkomycin Antibiotics†

David Venci, Guohua Zhao, and Marilyn Schuman Jorns*

Department of Biochemistry, Drexel University College of Medicine, Philadelphia, Pennsylvania 19102

Received August 5, 2002; Revised Manuscript Received October 8, 2002

ABSTRACT: Nikkomycin antibiotics are potent inhibitors of chitin synthase, effective as therapeutic antifungal agents in humans and easily degradable insecticides in agriculture. NikD is a novel flavoprotein that catalyzes the oxidation of Δ^1- or Δ^2-piperideine-2-carboxylate, a key step in the biosynthesis of nikkomycin antibiotics. The resulting dihydropicolinate product may be further oxidized by nikD or converted to picolinate in a nonenzymic reaction. Saturated nitrogen heterocycles (L-pipecolate, L-proline) and 3,4-dehydro-L-proline act as alternate substrates. The ability of nikD to oxidize 3,4-dehydro-L-proline, but not 1-cyclohexenoate, suggests that the enzyme is specific for the oxidation of a carbon−nitrogen bond. An equivalent reaction is possible with the enamine (Δ^2), but not the imine (Δ^1), form of the natural piperideine-2-carboxylate substrate. Apparent steady-state kinetic parameters for the reaction of nikD with Δ^1- or Δ^2-piperideine-2-carboxylate ($k_{cat} = 64$ min^{-1}; $K_m = 5.2$ μM) or 3,4-dehydro-L-proline ($k_{cat} = 18$ min^{-1}; $K_m = 13$ mM) were determined in air-saturated buffer by measuring hydrogen peroxide formation in a coupled assay. NikD appears to be a new member of the monomeric sarcosine oxidase (MSOX) family of amine oxidizing enzymes. The enzyme contains 1 mol of flavin adenine dinucleotide (FAD) covalently linked to Cys321. The covalent flavin attachment site and two residues that bind substrate carboxylate in MSOX are conserved in nikD. NikD, however, exhibits an unusual long-wavelength absorption band, attributed to charge-transfer interaction between FAD and an ionizable ($pK_a = 7.3$) active-site residue. Similar long-wavelength absorption bands have been observed for flavoproteins containing an active site cysteine or cysteine sulfenic acid. Interestingly, Cys273 in nikD aligns with an active-site histidine in MSOX (His269) that is, otherwise, a highly conserved residue within the MSOX family.

The enzyme nikD is postulated to catalyze a key step in the biosynthesis of nikkomycins (*1*, *2*). Nikkomycins are a closely related group of peptidyl nucleoside antibiotics that act as potent and specific competitive inhibitors of chitin synthase (*3*−*5*). Chitin, a homopolymer of N-acetyl-D-glucosamine, is important in maintaining the structural integrity of the cell walls of fungi and the exoskeleton of insects and other invertebrates. Chitin is not found in mammals. Nikkomycins are effective as therapeutic antifungal agents in humans and easily degraded insecticides in agriculture (*6*−*9*). Interest in nikkomycins has been especially spurred by the dramatic increase in the incidence of life-threatening fungal infections in humans owing to the increasing population of immunocompromised patients, such as AIDS victims, organ transplant recipients and cancer patients who receive chemotherapy.

Although the first bacterial strain identified as a producer of nikkomycins (*Streptomyces tendae* Tü901) was isolated in 1970, the biosynthesis of nikkomycins is only partially understood. The nucleoside and peptidyl moieties of nikkomycins are synthesized in separate pathways and then linked by a peptide bond (*10*). The synthesis of the peptidyl moiety is postulated to occur via a pathway involving nikD and 10 other enzymes, encoded by genes organized into two separate operons (*1*, *2*). Only the first enzyme in the pathway [L-lysine(-2-)aminotransferase, LAT] has actually been isolated and characterized (11). It has been demonstrated that LAT converts L-lysine to the corresponding 2-keto derivative, which spontaneously cyclizes and dehydrates to yield piperideine-2-carboxylate, a compound that can exist in both imine (Δ^1) and enamine (Δ^2) tautomeric forms. NikD is postulated to catalyze a four-electron oxidation of Δ^1- or Δ^2-piperideine-2-carboxylate to yield picolinate (eq 1), the second step in the proposed pathway for the synthesis of the peptidyl moiety of nikkomycin (*1*, *2*). Consistent with this proposal, nikkomycin synthesis in *S. tendae* Tü901 is blocked by inactivation of the gene encoding nikD and restored by adding picolinate (*1*).

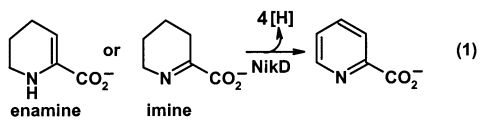

(1)

In this paper we report the first isolation and characterization of nikD. We show that nikD is a novel flavoprotein that exhibits many features in common with a recently recognized family of amine-oxidizing enzymes, named after the best characterized member, monomeric sarcosine oxidase

† This work was supported in part by Grant GM 31704 (M.S.J.) from the National Institutes of Health.

* To whom correspondence should be addressed: Phone (215) 762-7495; fax (215) 762-4452; e-mail marilyn.jorns@drexel.edu.

10.1021/bi020515y CCC: $22.00
Published on Web 12/07/2002

(MSOX).[1] All MSOX family members contain covalently bound flavin. Although exhibiting significant differences in substrate specificity, members of the MSOX family all oxidize an equivalent carbon−nitrogen bond (underlined) within a structural element [$R_1\underline{CH_2}$-$\underline{NH}CH(R_2)CO_2^-$] common to the various substrates (acyclic and cyclic α-amino acid derivatives) (*12*−*18*).

MATERIALS AND METHODS

Expression and Isolation of Recombinant NikD. A plasmid (pET19nikD) containing the *nikD* gene from *S. tendae* Tü901 was obtained as a generous gift from Christiane Bormann (University of Tübingen). PCR reactions were performed with PfuTurbo DNA polymerase (Stratagene), pET19nikD as template, and 5′-CACAGCAGCGGCCATATCGACGAC-3′ and 5′-TTTCCGGCGctcgagGAGAGCCGAC-3′ as forward and reverse primers, respectively [lowercase letters indicate mutations designed to eliminate the stop codon in the *nikD* gene and introduce a *Xho*I restriction site]. The PCR product was purified as previously described (*17*), cut, and ligated into the 5′-*Nde*I and 3′-*Xho*I sites of pET23a (Novagen) to yield plasmid pDV101. The sequence of the PCR product was verified by sequencing at the Nucleic Acid/Protein Research Core Facility of Children's Hospital of Philadelphia. *Escherichia coli* BL21(DE3) cells were transformed with plasmid pDV101 to carbenicillin resistance.

For large-scale nikD purification, 10 L of LB broth containing 0.1 mg/mL carbenicillin were inoculated with *E. coli* BL21(DE3)/pDV101 and incubated with shaking at 37 °C. Cultures were induced at $A_{595} = 0.6$ with 1 mM IPTG (Sigma) and harvested after 24 h. Cells were washed 3 times with 50 mM sodium phosphate buffer, pH 7.0, containing 500 mM NaCl, resuspended in 500 mL of lysis buffer [50 mM sodium phosphate buffer, pH 7.5, containing 500 mM NaCl, 20% glycerol, 0.25 mM $MgSO_4$, and a mixture of protease inhibitors and nucleases as previously described (*19*)], and then sonicated 20 times for 5 s, with 30 s intervals on ice. The cell lysate, obtained after centrifugation to remove debris, was adjusted to a protein concentration of 10 mg/mL, as determined by the Bio-Rad protein assay with bovine serum albumin as standard. The lysate was mixed with 25 mL of Talon metal affinity resin (Clontech), previously equilibrated with lysis buffer. The mixture was incubated for 1 h at 4 °C on a bidirectional orbital rocker. After being washed three times with wash buffer (50 mM sodium phosphate buffer, pH 7.5, containing 15 mM imidazole, 500 mM NaCl, and 20% glycerol), the resin was transferred to a column (20 × 1.5 cm) and washed a fourth time. NikD was eluted with a 1 L linear gradient from 0 to 150 mM imidazole in 50 mM sodium phosphate, pH 7.5, containing 500 mM NaCl and 20% glycerol. Fractions with a low A_{280}/A_{450} ratio (<9.0) were combined, concentrated, dialyzed against 50 mM sodium phosphate buffer, pH 8.0, and stored at −50 °C.

Flavin Analysis. The stoichiometry of flavin incorporation and the extinction coefficient at 455 nm was determined after denaturation with 3 M guanidine hydrochloride, as previously described (*14*). To determine the site of covalent flavin attachment, a sample of nikD (27.0 μg) was reductively alkylated with iodoacetamide by a procedure similar to that previously described (*14*). Promega modified sequencing-grade trypsin (0.4 μg) and chymotrypsin (0.1 μg) were added, and the mixture (29 μL) was digested overnight at 37 °C. An aliquot (2 μL) of the resulting peptide mixture was fractionated on an Hewlett-Packard 1100 HPLC system equipped with a capillary C18 reversed-phase (RP) column (L. C. Packing, 0.3 × 150 mm) by use of the following elution program at 0.125 mL/min: 0% solvent B, initial conditions; 10−130 min, linear gradient from 100% solvent A/0% solvent B to 67.5% solvent A/32.5% solvent B; then 130−169 min, 44.5% solvent A/55.5% solvent B; 169−170 min, 95% solvent B for column wash. Solvent A is 0.060% trifluoroacetic acid (TFA) in water. Solvent B is 0.043% TFA in acetonitrile. The HPLC was configured in a split-flow configuration, with the actual flow on the analytical column measured at 2.8 μL/min. The fused silica capillary outlet of the analytical column was lead directly to the 0.5 μL nanoflow cell in the diode array detector. Fractions were monitored during the gradient at 205 and 450 nm. Peaks were collected with a peak detection and collection apparatus (Isco model 2150 with Retriever II fraction collector) after a post-flow cell split-T, which was used to supplement the low flow for fraction collection. Fraction 52 absorbed at 450 nm and was sequenced by Edman degradation to determine the site of covalent flavin attachment. Sample digestion and analysis were conducted at the Harvard Microchemistry Laboratory.

For molecular weight determination, a sample of nikD was desalted by RP-HPLC and subjected to electrospray ionization mass spectral (ESI-MS) analysis, as detailed elsewhere (*20*). The data were used to discriminate between covalently bound flavin adenine dinucleotide (FAD) versus flavin mononucleotide (FMN).

Spectroscopy. Substrate reduction, photoreduction, and experiments to determine the effect of various ligands and pH on the nikD visible absorption spectrum were conducted by methods previously described (*13*, *21*). All experiments were conducted with commercially available reagents except for the Δ^1- or Δ^2-piperideine-2-carboxylate substrate (eq 1), which was synthesized and assayed as previously described (*11*, *22*). Solutions of Δ^1- or Δ^2-piperideine-2-carboxylate were prepared at pH 1.8 and neutralized immediately before use.

$$Y = \frac{AX}{X + K} \tag{2}$$

$$Y = \frac{AH^+ + BK_a}{H^+ + K_a} \tag{3}$$

Data Analysis. Data were fit to eqs 2 and 3 with the curve-fit function in Sigma Plot (Jandel Corp.). Equation 2 was used for analysis of spectrophotometric titration data for complexes formed with nikD and various ligands; Y and A are the observed and maximal absorbance change at the wavelength selected for analysis, respectively, X is the concentration of the varied ligand, and K is the complex dissociation constant. Equation 2 was also used to fit the steady-state kinetic data for the aerobic reaction of nikD with

[1] Abbreviations: MSOX, monomeric sarcosine oxidase; MTOX, *N*-methyltryptophan oxidase; MMTS, methylmethane thiosulfonate; EDTA, ethylenediaminetetraacetic acid; ESI-MS, electrospray ionization mass spectral; TFA, trifluoroacetic acid; IPTG, isopropyl thio-β-D-galactoside.

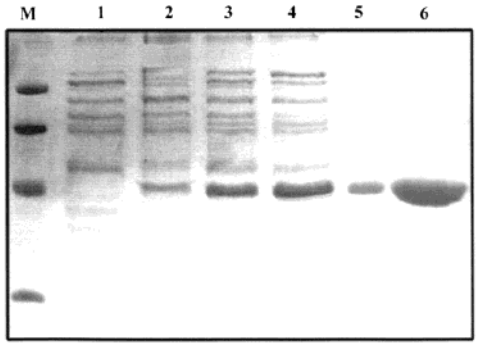

FIGURE 1: Expression of recombinant nikD. The SDS−15% polyacrylamide gel was stained for protein with Coomassie blue. Molecular markers (31, 45, 66, and 97 kDa) are shown in lane M. For lanes 1−4, *E. coli* BL21 (DE3) cells were transformed with empty vector (pET23a) or a derivative containing the *nikD* gene (pDV101). Cultures were induced at $A_{595} = 0.6$ with IPTG and harvested at various times, as indicated. Cell extracts were mixed with Talon metal affinity resin, the gel was washed with buffer, and bound proteins were eluted by boiling with 2% SDS for 3 min. Lane 1, empty vector, 24 h; lane 2, *nikD* vector, 0 h; lane 3, *nikD* vector, 2 h; lane 4, *nikD* vector, 24 h. Lanes 5 and 6 show 1 and 10 μg of pure nikD, isolated as described under Materials and Methods.

Δ^1- or Δ^2-piperideine-2-carboxylate and 3,4-dehydro-L-proline; Y and A are the observed and apparent maximal turnover rates, respectively, X is the substrate concentration, and K is the apparent K_m. Equation 3 was used to fit the effect of pH on the absorption spectrum of nikD. Y is the observed absorbance at a given wavelength and pH value. A and B are the calculated absorbance values at this wavelength at low and high pH values, respectively.

RESULTS AND DISCUSSION

Expression and Isolation of Recombinant NikD. NikD expression was not detected after transformation of *E. coli* BL21(DE3) cells with pET19nikD, a construct containing the *nikD* gene fused to an N-terminal $(His)_{10}$ tag. PCR was used to amplify the *nikD* gene, introduce a 3′-*Xho*I, site and mutate the stop codon to allow fusion with a C-terminal $(His)_6$ tag encoded by a pET23a vector. NikD expression was observed when the resulting construct (pDV101) was used to transform *E. coli* BL21(DE3) cells and reached a maximum level around 24 h after induction with IPTG (Figure 1). Pure nikD (~85 mg) was isolated from 10 L of cell culture in a single step on Talon metal affinity resin.

Flavin Analysis. The visible absorption spectrum of purified nikD exhibits two peaks ($\lambda_{max} = 455$, 379 nm, $\epsilon_{455} = 11\,200\ M^{-1}\ cm^{-1}$), characteristic of a flavin-containing enzyme (Figure 2, solid line 1). Analysis showed that nikD contained 0.9 mol of flavin/mol of protein. The nikD spectrum also exhibits an unexpected, long-wavelength absorption band. This band is eliminated upon denaturation with 3 M guanidine hydrochloride (Figure 2, solid line 2), suggesting that it might be due to a charge-transfer complex that is stabilized by the native protein structure.

The yellow flavin color of a solution containing denatured nikD was found in the retentate after microfiltration, indicating that the flavin was covalently bound to the protein, a characteristic feature of the MSOX family. To determine whether the covalent flavin in nikD was present as FAD or FMN, nikD was subjected to ESI-MS analysis. The analysis

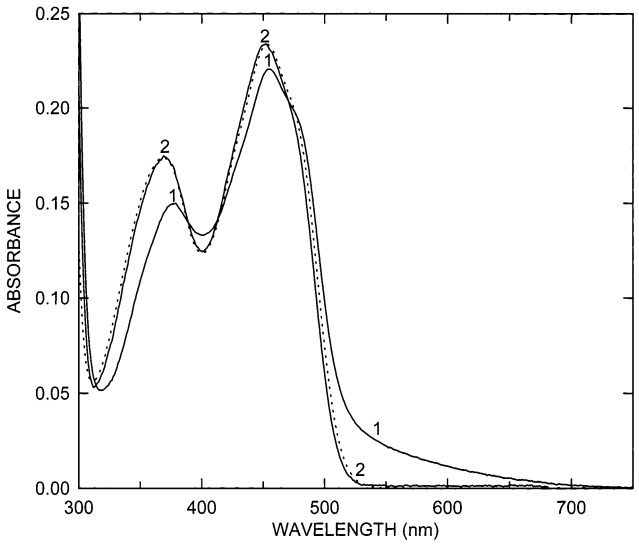

FIGURE 2: Effect of denaturation on the absorption spectrum of nikD. Curve 1 (solid line) shows the absorption spectrum of native nikD in 50 mM potassium phosphate buffer, pH 8.0 at 25 °C. Curve 2 (solid line) was recorded after denaturation of nikD with 3 M guanidine hydrochloride. For comparison, the dotted line shows the spectrum obtained after denaturation of MSOX with 3 M guanidine hydrochloride and normalization to the same A_{450} as the denatured nikD sample.

indicated the presence of a major component with an observed mass (44 908.5 ± 6.8 amu) that corresponds to the mass calculated for nikD apoenzyme plus FAD (44 904 amu). A secondary peak at 45 018.5 ± 7.0 amu most likely corresponds to the TFA adduct of the same species (45 018 amu). An additional secondary peak (44 776 ± 7.0 amu) is probably due to removal of the N-terminal Met from the major species (44 773 amu). A species corresponding to the FMN form of the major peak (44 574 amu) was not detected. The results indicate that nikD contains covalently bound FAD, as observed for MSOX and *N*-methyltryptophan oxidase (MTOX), another member of the MSOX family (*14*).

To determine the site of covalent flavin attachment, a chymotrypsin/trypsin digest was prepared and fractionated by HPLC. Fractions were monitored for peptide and flavin absorption at 205 and 450 nm, respectively. Fraction 52 absorbed at 450 nm and was selected for Edman degradation. This fraction was not well resolved from neighboring fractions. More than one peptide sequence was expected and observed. Fraction 52 contained two copurifying peptides. The flavin-containing peptide was the secondary component, as judged by the fact that no identifiable amino acid was detected in the fourth cycle of its Edman degradation. The observed sequence, ^{318}TSTXLAVLPTDP^{329}, begins with a tryptic cleavage site and coincides with residues 318−329 in the nikD sequence. The "missing" amino acid in the fourth cycle coincides with Cys321, a residue that aligns with the known covalent flavin attachment site in MSOX and MTOX (Figure 3, bottom panel) (*14*). (Since the nikD sample was alkylated with iodoacetamide prior to analysis, nonflavinylated cysteines will yield an observable PTH-CAM-Cys during Edman degradation.) An identifiable amino acid was obtained in each cycle for the primary peptide in fraction 52 (^{258}YGFGHNP^{264}). The sequence of this peptide begins with a chymotryptic site and coincides with residues 258−264 (Figure 3, top panel). The results indicate that nikD

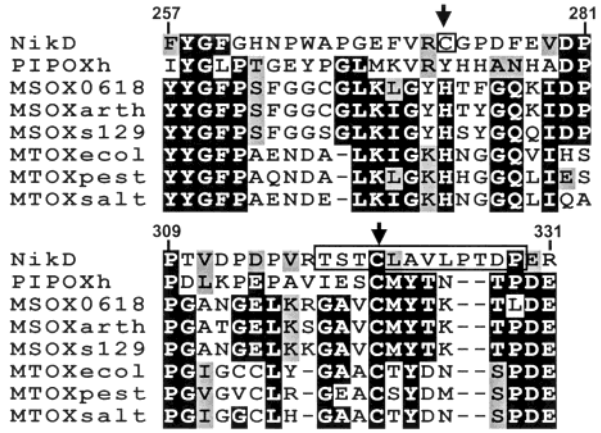

FIGURE 3: Multiple sequence alignment of nikD with various MSOX family members, including human pipecolate oxidase (PIPOXh); MSOX from *Bacillus* sp. 0618 (MSOX0618), *Arthrobacter* TE-1826 (MSOXarth), or *Bacillus* sp. NS129 (MSOXs129); and MTOX from *E. coli* (MTOXecol), *Yersinia pestis* (MTOXpest) or *Salmonella typhimurium* (MTOXsalt). The top segment shows that Cys273 in nikD (boxed) aligns with a highly conserved active-site histidine in MSOX and MTOX. The bottom segment shows that Cys321 in nikD aligns with a highly conserved cysteine that serves as the covalent flavin attachment site in MSOX and MTOX. The boxed region corresponds to the sequence of the flavin peptide isolated from a proteolytic digest of nikD.

contains FAD covalently linked to Cys321. There are two known types of covalent flavin linkages involving a cysteinyl residue. A 6-*S*-cysteinyl linkage can be ruled out since these flavin derivatives exhibit a single absorption band in the visible region [$\lambda_{max} = 437$ nm for 6-(*S*-cysteinyl)riboflavin)] (*23*). The absorption spectrum observed for the nikD flavin after denaturation of the enzyme with guanidine hydrochloride ($\lambda_{max} = 450$, 369 nm) resembles that reported for 8α-*S*-cysteinylriboflavin ($\lambda_{max} = 448$, 367 nm) (*24*) and virtually superimposes with a spectrum recorded after denaturation of MSOX (Figure 2, dotted curve). The results indicate that an 8α-*S*-cysteinyl linkage is likely for the nikD flavin, the same linkage reported for MSOX and MTOX (*14*).

Identification of New NikD Substrates and Inhibitors. The flavin in nikD is converted to a two-electron reduced form immediately upon mixing the enzyme (14.2 μM) under anaerobic conditions with a 10-fold excess of Δ^1- or Δ^2-piperideine-2-carboxylate (150 μM), as judged by the characteristic bleaching of the oxidized flavin spectrum in a reaction that is also accompanied by the loss of the long-wavelength absorption band (Figure 4A). Similar results are obtained upon reaction with a stoichiometric amount (14.3 μM) of Δ^1- or Δ^2-piperideine-2-carboxylate (data not shown). The results show that nikD can efficiently catalyze at least a two-electron oxidation of the proposed physiological substrate.

Alternate substrates for nikD were identified by conducting similar anaerobic spectral experiments with various analogues of the physiological substrate (Table 1). L-Pipecolate acts as an alternate substrate, indicating that the double bond in the natural substrate is not essential. NikD will also oxidize nitrogen heterocycles containing a five-membered ring, as judged by the results obtained with L-proline and 3,4-dehydro-L-proline. Unlike the physiological substrate, these alternate substrates are oxidized in relatively slow reactions, a feature that allowed us to monitor the complete spectral

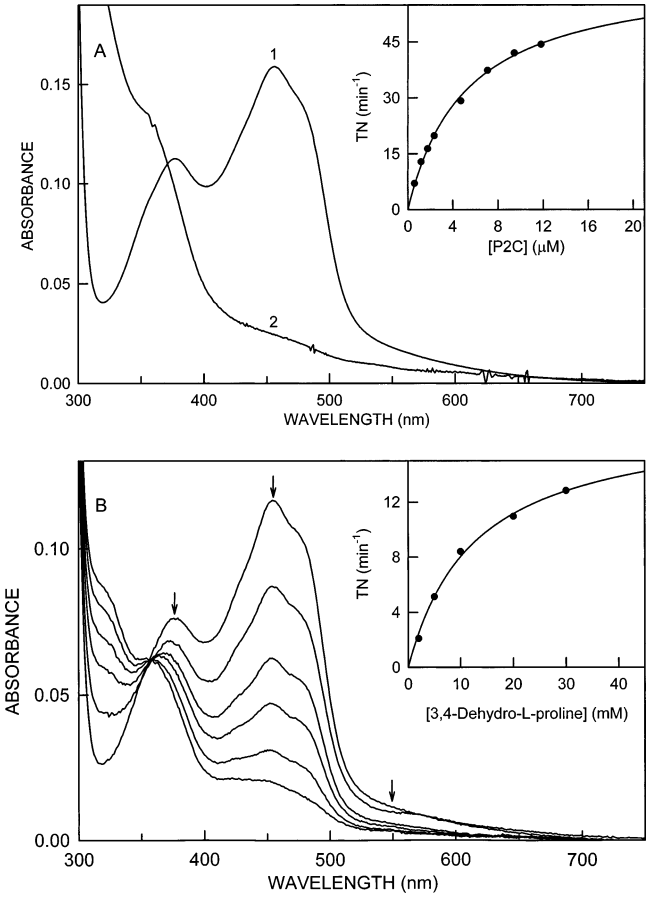

FIGURE 4: Reduction of nikD with Δ^1- or Δ^2-piperideine-2-carboxylate or 3,4-dehydro-L-proline. Except as indicated, reactions were conducted under anaerobic conditions in 50 mM potassium phosphate buffer, pH 8.0 at 4 °C. Panel A shows spectra recorded before (curve 1) and immediately after (curve 2) mixing nikD (14.2 μM) with 150 μM Δ^1- or Δ^2-piperideine-2-carboxylate. Panel B shows spectra recorded before and 1, 4, 10, 20, and 42 min after mixing nikD (10.4 μM) with 100 μM 3,4-dehydro-L-proline. Arrows indicate the direction of the spectral changes. The insets to panels A and B are plots of the rate of turnover of nikD as a function of the concentration of Δ^1- or Δ^2-piperideine-2-carboxylate (P2C) or 3,4-dehydro-L-proline, respectively. Reactions were conducted under aerobic conditions at 25 °C, as described in Table 2. The solid lines are fits of the data (●) to eq 2.

course of the reduction of nikD in manual mixing experiments, as illustrated by the reaction observed with 100 μM 3,4-dehydro-L-proline at 4 °C (Figure 4B). Under these conditions, the reaction with 3,4-dehydro-L-proline exhibited apparent first-order kinetics ($k_{obs} = 0.096$ min^{-1}) and an isosbestic conversion of the oxidized flavin to 1,5-dihydro-FAD, accompanied by the loss of the long-wavelength absorption band. The reactions with all substrates tested were immediately reversible upon aeration of the samples.

The identification of 3,4-dehydro-L-proline as an alternate substrate for nikD may be of mechanistic significance. Unlike other substrates, 3,4-dehydro-L-proline can only undergo a two-electron oxidation in a reaction that must involve oxidation of a carbon−nitrogen bond rather than a carbon−carbon bond. Oxidation of either of the two carbon−nitrogen bonds in 3,4-dehydro-L-proline will yield an unstable tautomer (Scheme 1, path A or B) that rearranges to yield the stable aromatic tautomer, pyrrole-2-carboxylate. The reaction shown in path B obeys the substrate specificity pattern exhibited by various members of the MSOX family with

Table 1: Identification of New nikD Substrates and Inhibitors

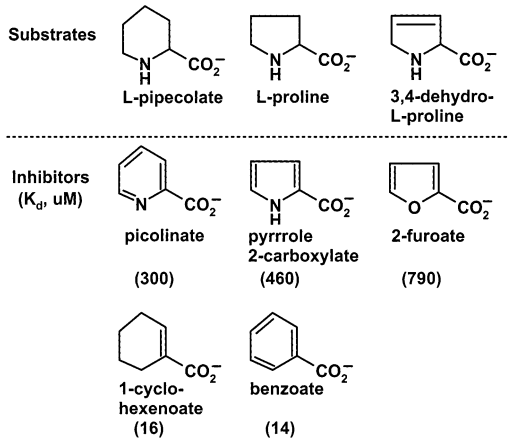

Scheme 1 : Two Possible Paths for the nikD-Catalyzed Conversion of 3,4-Dehydro-L-proline to Pyrrole-2-carboxylate

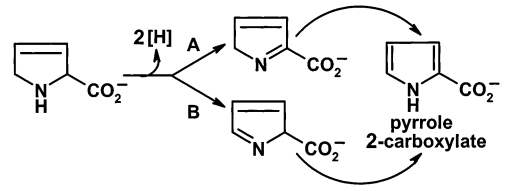

physiological or alternate substrates (*16*, *21*, *25*, *26*) and is the reaction observed with MSOX and 3,4-dehydro-L-proline.[2] Oxidation of a carbon−nitrogen bond, equivalent to that shown in path B for the 3,4-dehydro-L-proline reaction, is feasible with the enamine form of the physiological substrate for nikD (eq 1). With the imine form, only oxidation of carbon−carbon bonds is possible. Interestingly, calculations by Nishina et al. (*27*) indicate that the enamine would be more easily oxidized than the imine.

Additional evidence suggesting that nikD oxidizes the carbon−nitrogen bond in the enamine form of piperideine-2-carboxylate is provided by the fact that analogues lacking a ring nitrogen are not oxidized by nikD. For example, 1-cyclohexenoate is not a substrate although the compound is tightly bound at the active site of nikD (Table 1). Other inhibitors include benzoate, picolinate (the proposed product of the physiological reaction), pyrrole-2-carboxylate (the product of the nikD reaction with 3,4-dehydro-L-proline), and 2-furoate (Table 1). Binding constants for these inhibitors were determined on the basis of the perturbation of the visible absorption spectrum of nikD, as illustrated by the titration with picolinate shown in Figure 5. Although the observed spectral perturbation varied depending on the inhibitor, the binding of all inhibitors resulted in the loss of the long-wavelength absorption band of uncomplexed nikD.

Photoreduction of NikD. The flavin in nikD is reducible by photoreduction in the presence of 5-deazariboflavin, methyl viologen, and EDTA. Unlike substrate reduction, photoreduction of nikD occurs in two phases and appears to proceed via a radical intermediate. Conversion of oxidized enzyme to the radical form results in loss of absorption at

[2] M. A. Wagner and M. S. Jorns, unpublished results.

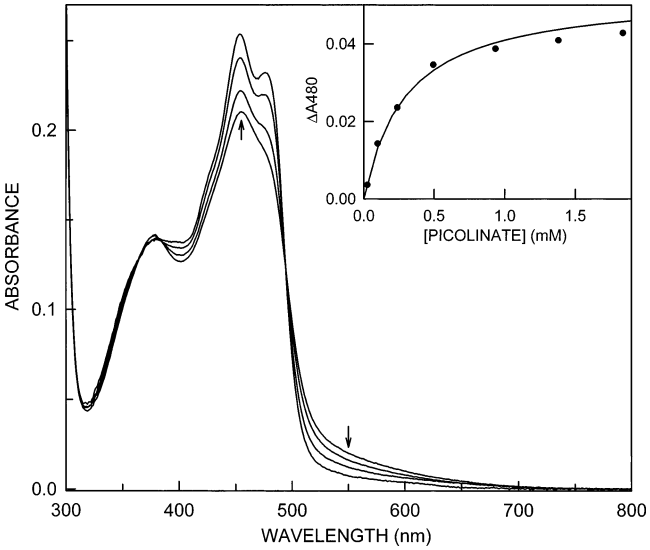

FIGURE 5: Titration of nikD with picolinate. The titration was performed in 50 mM potassium phosphate buffer, pH 8.0 at 25 °C. The direction of spectral changes is indicated by arrows. Spectra were recorded in the presence of 0, 98, 496, and 2270 μM picolinate (in that order at the arrows). The inset shows a fit (solid line) of the observed increase in absorption at 480 nm (●) to a theoretical binding curve (eq 2).

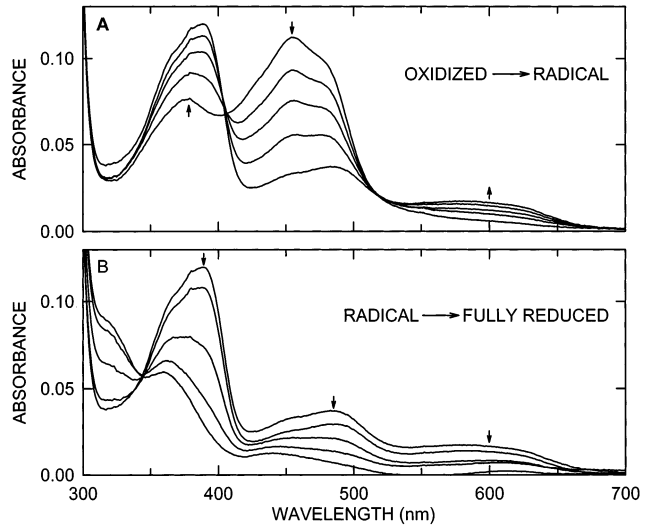

FIGURE 6: Anaerobic photoreduction of nikD in 50 mM potassium phosphate buffer, pH 8.0, containing 1 μM 5-deazariboflavin, 2 μM methyl viologen, and 120 μM EDTA at room temperature. Arrows indicate the direction of spectral changes. Panel A shows the conversion of oxidized enzyme to the flavin radical form, recorded after irradiation for 0, 10, 20, 30, and 50 s. Panel B shows the reduction of the radical to fully reduced flavin, recorded after irradiation for 50, 60, 80, 100, and 110 s.

450 nm, accompanied by increases around 390 nm (Figure 6A), spectral changes consistent with the formation of a red, anionic radical, as observed with MSOX, MTOX, and various other flavoprotein oxidases (*13*, *18*, *28*). This phase of the nikD reaction, however, also results in modest absorption increases at 600 nm, a feature generally observed only with formation of a blue neutral radical. In the second phase of the photoreduction of nikD, the radical mixture is converted to fully reduced, 1,5-dihydroflavin (Figure 6B). As with substrate reduction, the long-wavelength absorption band of oxidized nikD is eliminated upon photoreduction and the observed spectral changes are fully reversible upon

Table 2: Steady-State Kinetic Parameters[a]

enzyme	substrate	$k_{cat(app)}$ (min^{-1})	$K_{m(app)}$ (μM)	k_{cat}/K_m (M^{-1} min^{-1})
nikD	Δ^1- or Δ^2-piperideine-2-carboxylate	64 ± 2	5.2 ± 0.3	1.2×10^7
MSOX	sarcosine	2730 ± 32	4500 ± 100	6.1×10^5
nikD	3,4-dehydro-L-proline	18 ± 1	13000 ± 2000	1.4×10^3

[a] Apparent steady-state kinetic parameters were determined in air-saturated buffer (100 mM potassium phosphate, pH 8.0, at 25 °C) by a horseradish peroxidase-coupled assay (*21*). The values for MSOX were taken from Wagner and Jorns (*21*).

aeration. The observed facile reoxidation reactions suggest that oxygen may be the natural electron acceptor for nikD.

Turnover of NikD with Δ^1- or Δ^2-Piperideine-2-carboxylate. Reaction of nikD with Δ^1- or Δ^2-piperideine-2-carboxylate under aerobic conditions is accompanied by the reduction of oxygen to hydrogen peroxide, as expected for a member of the MSOX family of amine oxidases. Formation of hydrogen peroxide was monitored in a horseradish peroxidase-coupled assay (*21*) in air-saturated buffer. The reaction exhibits saturation kinetics, as judged by the fit of the rates observed at various concentrations of Δ^1- or Δ^2-piperideine-2-carboxylate to a Michaelis−Menten equation (Figure 4A, inset). Table 2 compares the apparent steady-state kinetic parameters for the nikD reaction with Δ^1- or Δ^2-piperideine-2-carboxylate to those observed for MSOX reaction with sarcosine under the same conditions. The apparent turnover rate of nikD is about 40-fold slower than observed with MSOX. The apparent K_m of nikD for its physiological substrate is, however, about 1000-fold smaller than observed for the corresponding K_m in the MSOX reaction. As a result, the apparent catalytic efficiency of nikD is 20-fold greater than observed with MSOX ($k_{cat(app)}/K_{m(app)} = 1.2 \times 10^7$ versus 6.1×10^5 M^{-1} min^{-1}). The efficiency of the nikD reaction at low substrate concentrations suggests an evolutionary adaptation designed to prevent cellular accumulation of piperideine-2-carboxylate, a relatively unstable compound under physiological conditions. As discussed by Northrop (*29*), bacterial enzymes responsible for antibiotic resistance employ a similar strategy to keep the antibiotic concentration as low as possible. These enzymes exhibit modest values for k_{cat} but large values for k_{cat}/K_m, as observed for nikD. These examples are in keeping with Northrop's proposal that k_{cat}/K_m provides a measure of an enzyme's ability to *capture* the substrate absolutely, committing it to a turnover (*29*).

Turnover of NikD with 3,4-Dehydro-L-proline. As observed with the physiological substrate, turnover of nikD with 3,4-dehydro-L-proline in air-saturated buffer exhibits saturation kinetics (Figure 4B, inset) and is accompanied by the reduction of oxygen to hydrogen peroxide. The apparent turnover rate with 3,4-dehydro-L-proline is only 4-fold slower than with Δ^1- or Δ^2-piperideine-2-carboxylate, but the apparent K_m is more than 3 orders of magnitude larger. Consequently, the apparent catalytic efficiency with 3,4-dehydro-L-proline is decreased by 4 orders of magnitude as compared with the physiological substrate (Table 2).

Effect of pH on the NikD Absorption Spectrum. The spectral experiments described above were conducted at pH 8.0. Additional studies show that the absorption spectrum of nikD in the oxidized state is markedly pH-dependent.

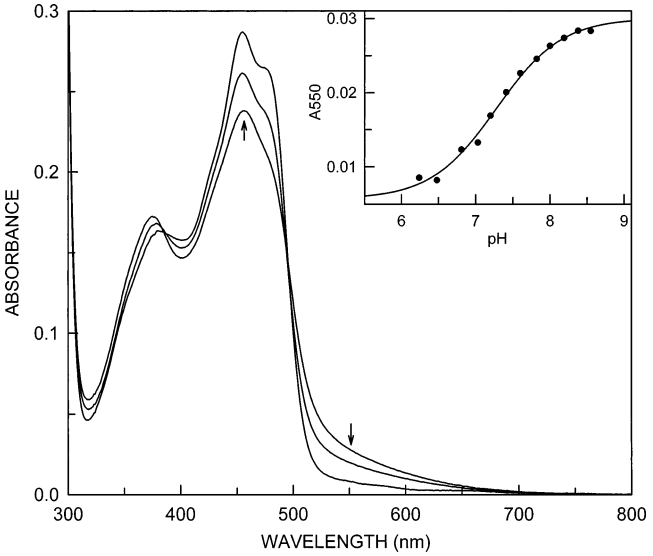

FIGURE 7: pH titration of nikD. Spectra were recorded at pH 8.55, 7.41, and 6.48 in 100 mM potassium phosphate buffer at 25 °C. The arrows indicate the direction of absorbance change as the pH is lowered. The inset shows a fit (solid line) of the observed absorbance change at 550 nm (●) to a theoretical pH titration curve (eq 3).

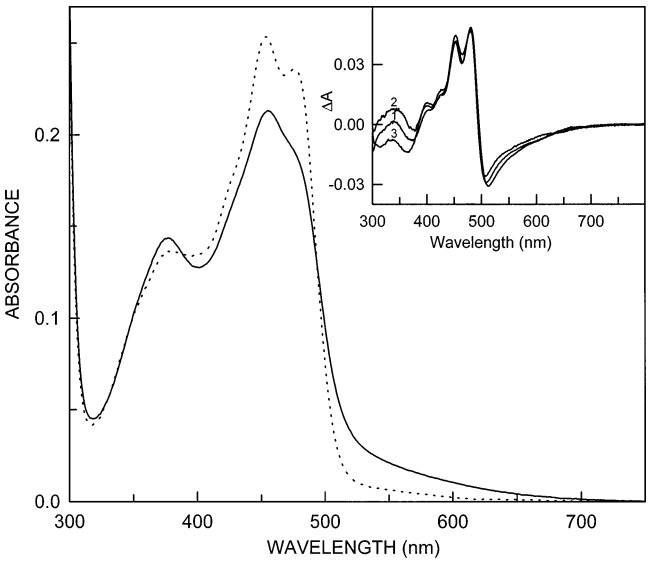

FIGURE 8: Effect of MMTS on the absorption spectrum of nikD. The solid line shows the absorption spectrum of untreated nikD in 50 mM potassium phosphate buffer, pH 8.0, at 20 °C. The spectrum shown by the dotted line was recorded 15 min after addition of 10 mM MMTS. The inset shows difference spectra calculated for the MMTS reaction (curve 1), complex formation with picolinate (curve 2), and a decrease in pH from 8.55 to 6.48 (curve 3). The difference spectra are normalized to the same protein concentration.

Spectra obtained upon dilution of a nikD stock solution into 100 mM phosphate buffers at various pH values show that the long-wavelength absorption band disappears as the pH is decreased in an isosbestic reaction, accompanied by an increase in absorption at 455 nm (Figure 7). The spectral changes observed upon acidification closely resemble those observed upon titration of nikD with picolinate (see Figure 5 and Figure 8, inset). Analysis of nikD absorbance changes at 550 nm (or other wavelengths) as a function of pH yields a pK_a value of 7.3 (Figure 7, inset).

The Long-Wavelength Absorption Band. As described above, the nikD long-wavelength absorption band can be

eliminated by enzyme denaturation, substrate reduction, photoreduction, inhibitor binding, and weakly acidic pH. The long-wavelength band is apparently due to a charge-transfer interaction with the oxidized flavin as acceptor and an amino acid residue or a tightly bound ligand as donor. Denaturation disrupts the close contact required for charge-transfer interaction. The charge-transfer interaction is disrupted by reduction since the reduced flavin is not electron deficient and cannot act as a charge-transfer acceptor. The pH effect suggests that charge-transfer interaction can occur only when an ionizable group in the donor is unprotonated. Enzyme inhibitors might displace another active-site ligand or sterically block interaction of the flavin with an amino acid residue. To distinguish between these two possibilities, nikD was mixed with 2.0 mM picolinate to disrupt the charge-transfer complex. The sample was then subjected to several cycles of microfiltration to remove any displaced ligand and then to remove picolinate. The absorption spectrum of the treated enzyme was superimposed with an untreated control (data not shown). The results indicate that the charge-transfer donor is likely to be an active-site amino acid residue. Three observations suggest that the charge-transfer donor might be a cysteine residue: (I) Our studies show that His269 in MSOX is at the active site and plays an important role in catalysis (*12*, *13*, *30*). This residue is highly conserved in other members of the MSOX family except for nikD, where it is replaced by Cys273 (Figure 3, top panel). (His269 in MSOX aligns with a tyrosine residue in pipecolate oxidase, but two histidine residues are immediately C-terminal to this tyrosine.) (II) Active-site cysteine residues in other flavoenzymes are known to form charge-transfer complexes with oxidized flavin. The absorption spectrum of native nikD is strikingly similar to that reported for NADH oxidase from *Enterococcus faecalis*, an enzyme that exhibits charge-transfer interaction between FAD and Cys42, in its thiol form and also as the corresponding cysteine sulfenic acid (*31*). (III) Methylmethane thiosulfonate (MMTS) is best known as a reagent for modifying sulfhydryl groups (CysSH → $CysSSCH_3$) but produces an analogous modification with cysteine sulfenic acid [CysSOH → $CysS(=O)SCH_3$] (*32*). Significantly, the long-wavelength absorption band in nikD is eliminated upon reaction with MMTS (Figure 8). The calculated difference spectrum for the MMTS reaction is very similar to the perturbation elicited by picolinate binding or by weakly acidic pH (Figure 8, inset).

Conclusions. NikD is a novel flavoprotein that is important in the biosynthesis of nikkomycin antibiotics. In addition to the natural substrate (Δ^1- or Δ^2-piperideine-2-carboxylate), nikD will oxidize saturated nitrogen heterocycles containing a six-membered (L-pipecolate) or five-membered (L-proline) ring. The ability of the enzyme to oxidize 3,4-dehydro-L-proline, but not 1-cyclohexenoate, suggests that nikD is specific for the oxidation of a carbon−nitrogen bond. An equivalent reaction is possible with the enamine (Δ^2), but not the imine (Δ^1), form of the natural substrate. While the results clearly demonstrate that nikD catalyzes a facile two-electron oxidation of piperideine-2-carboxylate, it is not known whether the resulting dihydropicolinate product is further oxidized by nikD or subject to a nonenzymic disproportionation or oxidative conversion to picolinate.

NikD appears to be a new member of the MSOX family of amine-oxidizing enzymes. Although the vast majority of flavoenzymes contain noncovalently bound flavin, all members of the MSOX family contain covalently bound flavin (*12*−*18*). Recombinant nikD is found to contain 1 mol of FAD covalently linked to Cys321, probably via a thioether bond to the 8α position of FAD, the same linkage observed for two other members of the MSOX family (*14*). NikD exhibits 25% sequence identity with MSOX, a value that falls within the range (23−43% identity) observed for other MSOX family members. Six active-site residues in MSOX (Arg49, Arg52, Tyr55, Tyr254, Cys315, and Lys348) (*12*) are conserved in nikD (Arg50, Arg53, Tyr56, Tyr258, Cys321, and Lys358), including the covalent flavin attachment site (Cys321) and two residues known to bind substrate carboxylate in MSOX (Arg53 and Lys358). MSOX and nikD exhibit overlapping substrate specificity, as judged by the fact that three compounds identified as alternate substrates for nikD (L-pipecolate, L-proline, and 3,4-dehydro-L-proline) are also oxidized by MSOX (*26*).[2]

Unlike other MSOX family members, nikD exhibits an unusual long-wavelength absorption band, that is likely due to charge-transfer interaction between oxidized FAD and a Cys-thiolate moiety at the active site. The Cys-thiolate is tentatively attributed to Cys273, a residue that aligns with an active-site histidine (His269) in MSOX that is conserved in other members of the MSOX family. The nikD absorption spectrum resembles that observed for NADH oxidase, where the long-wavelength band is due to charge-transfer interaction between FAD and Cys42 (*31*). Cys42 functions as a second redox-active group in NADH oxidase, cycling between sulfenic (CysSOH) and sulfhydryl (CysSH) oxidation states in resting and transiently reduced enzyme, respectively. No reaction is, however, observed upon mixing nikD with 5-thio-2-nitrobenzoic acid, a specific reagent for CysSOH (*32*).[3] The role of Cys273 in nikD catalysis is currently under investigation.

ACKNOWLEDGMENT

Plasmid pET19nikD containing the *nikD* gene was obtained as a generous gift from Christiane Bormann (University of Tübingen). We thank Franta Hubalek (Emory University) for performing the ESI-MS analysis.

REFERENCES

1. Bruntner, C., Lauer, B., Schwarz, W., Mohrle, V., and Bormann, C. (1999) *Mol. Gen. Genet. 262*, 102−114.
2. Lauer, B., Russwurm, R., Schwarz, W., Kalmanczhelyi, A., Bruntner, C., Rosemeier, A., and Bormann, C. (2001) *Mol. Gen. Genet. 264*, 662−673.
3. Brillinger, G. U. (1979) *Arch. Microbiol. 121*, 71−74.
4. Dahn, U., Hagenmaier, H., Hohne, H., Konig, W. A., Wolf, G., and Zahner, H. (1976) *Arch. Microbiol. 107*, 143−160.
5. Fiedler, H.-P., Kurth, R., Langharig, J., Delzer, J., and Zahner, H. (1982) *J. Chem. Biotechnol. 32*, 271−280.
6. Hector, R. F., Zimmer, B. L., and Pappagianis, D. (1990) *Antimicrob. Agents Chemother. 34*, 587−593.
7. Hector, R. F., and Schaller, K. (1992) *Antimicrob. Agents Chemother. 36*, 1284−1289.
8. Zhang, D., and Miller, M. J. (1999) *Curr. Pharm. Des. 5*, 73−99.
9. Hector, R. F. (1993) *Clin. Microb. 6*, 1−21.
10. Bormann, C., Mattern, S., Schrempf, H., Fiedler, H. P., and Zahner, H. (1989) *J. Antibiot. 42*, 913−918.
11. Bruntner, C., and Bormann, C. (1998) *Eur. J. Biochem. 254*, 347−355.

[3] D. Venci and M. S. Jorns, unpublished results.

12. Trickey, P., Wagner, M. A., Jorns, M. S., and Mathews, F. S. (1999) *Structure 7*, 331−345.
13. Wagner, M. A., Trickey, P., Chen, Z., Mathews, F. S., and Jorns, M. S. (2000) *Biochemistry 39*, 8813−8824.
14. Wagner, M. A., Khanna, P., and Jorns, M. S. (1999) *Biochemistry 38*, 5588−5595.
15. Chlumsky, L. J., Zhang, L., and Jorns, M. S. (1995) *J. Biol. Chem. 270*, 18252−18259.
16. Reuber, B. E., Karl, C., Reimann, S. A., Mihalik, S. J., and Dodt, G. (1997) *J. Biol. Chem. 272*, 6766−6776.
17. Eschenbrenner, M., Chlumsky, L. J., Khanna, P., Strasser, F., and Jorns, M. S. (2001) *Biochemistry 40*, 5352−5367.
18. Khanna, P., and Jorns, M. S. (2001) *Biochemistry 40*, 1441−1450.
19. Kvalnes-Krick, K., and Jorns, M. S. (1986) *Biochemistry 25*, 6061−6069.
20. Li, M., Hubalek, F., Newton-Vinson, P., and Edmondson, D. E. (2002) *Protein Expression Purif. 24*, 152−162.
21. Wagner, M. A., and Jorns, M. S. (2000) *Biochemistry 39*, 8825−8829.
22. Nishina, Y., Sato, K., Shi, R. W., Setoyama, C., Miura, R., and Shiga, S. (2001) *J. Biochem. (Tokyo) 130*, 637−647.
23. Steenkamp, D. J., McIntire, W., and Kenney, W. C. (1978) *J. Biol. Chem. 253*, 2818−2824.
24. Walker, W. H., Kearney, E. B., Seng, R. L., and Singer, T. P. (1971) *Eur. J. Biochem. 24*, 328−331.
25. Khanna, P., and Jorns, M. S. (2001) *Biochemistry 40*, 1441−1450.
26. Zeller, H.-D., Hille, R., and Jorns, M. S. (1989) *Biochemistry 28*, 5145−5154.
27. Nishina, Y., Sato, K., and Shiga, K. (1991) *J. Biochem. (Tokyo) 109*, 705−710.
28. Massey, V., Muller, F., Feldberg, R., Schuman, M., Sullivan, P. A., Howell, L. G., Mayhew, S. G., Matthews, R. G., and Foust, G. P. (1969) *J. Biol. Chem. 244*, 3999−4006.
29. Northrop, D. B. (1998) *J. Chem. Educ. 75*, 1153−1157.
30. Zhao, G, Song, H., Chen, Z., Mathews, F. S., and Jorns, M. S. (2002) *Biochemistry 41*, 9751−9764.
31. Mallett, T. C., and Claiborne, A. (1998) *Biochemistry 37*, 8790−8802.
32. Poole, L. B., and Ellis, H. R. (2002) *Methods Enzymol. 348*, 122−136.

BI020515Y